MECHANISM OF NANOFRAGMENT FORMATION IN $A_2^V B_3^{VI}$-TYPE CRYSTALS

K.Sh. GAHRAMANOV [1], S.Sh. GAHRAMANOV[1], N.A. ABDULLAYEV[1,2],
Kh.V. ALIGULIYEVA[3], Z.I. BADALOVA[1], H.V. ORUJOVA[1], A.A. BADALOV[1]
[1]Institute of Physics, National Academy of Sciences of Azerbaijan
H. Javid ave.131, AZ1143 Baku, Azerbaijan
[2]Baku State University, Z. Xalilov str., 33, AZ1148 Baku, Azerbaijan
[3]Sumgait State University, 43th district, Baku str., 1, AZ5008 Sumgait, Azerbaijan
e-mail: samir.gahramanov@gmail.com

Ways to improve the degree of ordering of self-organized nanoobjects in $A_2^V B_3^{VI}$<impurity> systems are discussed. It is shown that, as a result of diffusion intercalation during crystal growth, it is possible to combine the methods of vertical directional crystallization with additional migration of atoms *(*Cu, Ni, Zn, In, Se*,)* into the interlayer space and defect cavities. Apparently, stress relaxation between quintets occurs through the mechanisms of elastic and plastic deformation with mass transfer and the appearance of screw dislocations, which affects the nature of folded-corrugated submicrostructures and the distribution density of nanoislands. Nanoislands and fold formations are evidenced by AFM images in 2*D* and 3*D* scales.

Keywords: layered crystals, plastic deformation, mass transfer, self-organized nanoobjects, corrugated microstructures.
PACS: 61.46.Df; 61.72.−y; 61.72.Cc

It is well known that the processes of elastic and plastic deformation of metal and semiconductor films on substrates during growth and mechanical loading are of interest in revealing the role of the periodic distribution of stresses and strains at the interface between two-layer systems. When such films are compressed on a pliable substrate, folds (corrugations) are formed on their surface and a coherent deformation of the substrate occurs. In the case of a rigid substrate, compressive stresses lead to elastic bending of the film with local or periodic delamination from the substrate. In this case, it is also necessary to take into account the movement of mass by plastic shear this process can determine the change in the shape of deformable bodies and their elements. The processes associated with the movement of atoms within the interlayer space of layered crystals can be called mass transfer. If there is a density gradient in the crystal or a mass gradient in it, excitations of cooperative displacements of atoms are possible. Shear displacements can develop along crystallographic planes, along grain boundaries, and also arise due to inhomogeneous slip along crack surfaces.

The analysis carried out in [1] of various types of deformation developing under the action of compressive stresses in thin films, as well as some of the conclusions drawn, can be considered as a model for a van der Waals surface and in layered crystals. This is due to the formation of a periodic folded relief on the surface of the films, as well as between the layers in $A_2^V B_3^{VI}$, and as shown in [1], the wavelength and amplitude of the folds are determined by the competition between the energy and kinetics of the film and substrate deformation processes. The periodic nature of the deformation of a thin film leads to a periodic distribution of normal and shear stresses in the "film-substrate" system. Depending on the loading conditions and the ratio of the characteristics of the film and substrate, stress relaxation occurs through elastic and plastic deformation: local or periodic delamination of the film from the substrate, the formation of wrinkles, the disintegration of the film into separate islands, etc. Corrugation of structures occurs only when a certain critical compressive stress is exceeded [2–3]:

$$\sigma_w = \frac{\overline{E}_f}{4} \left(\frac{3\overline{E}_s}{\overline{E}_f}\right) 2/3 \qquad (1)$$

where $\overline{E}_f = E_f (1–V^2_f)$ and $\overline{E}_s = E_s/(1–V^2_s)$ are the modulus of longitudinal elasticity of the film and substrate, respectively. When the compressive stress σ exceeds σ_w, the film spontaneously bends, forming a periodic distribution of folds on the surface. Each wrinkle in a family with a fixed amplitude-to-wavelength ratio attenuates stresses by the same amount. The wavelength and amplitude of the folds A are determined by the energy of the process, i.e. the ratio between the change in the energy of elastic compression of the film and the sum of the energies of elastic bending of the film and substrate [3–4].

$$\lambda = 2\pi h \left(\frac{\overline{E}_f}{3\overline{E}_s}\right)^{\frac{1}{3}} \qquad (2)$$

$$A = h\sqrt{\frac{\sigma}{\sigma_w}} \qquad (3)$$

where h is the film thickness. The formation of wrinkles with a long wavelength is energetically unfavorable due to an increase in the strain energy of the substrate, and wrinkles with a short wavelength lead to a large bending energy of the film. Therefore, the need to minimize the total elastic energy leads to the formation of medium-sized folds. As can be seen from (2), in the case of an elastic substrate, the wrinkle wavelength is determined by the elastic characteristics of the film and substrate, as well as by the film thickness. Moreover, it does not depend on the magnitude of stresses, i.e. is a constant value for

the "film-substrate" system. On the contrary, the wrinkle amplitude does not depend on the elastic properties of the film and substrate, but increases with increasing compressive stresses. Here, it is also necessary to study the effect of growth conditions not only on the morphology of the interlayer space, but also on the thermoelectric parameters of $A_2^V B_3^{VI}$. Microinhomogeneities are formed during crystallization: as a result, an inhomogeneous columnar or layered structure is created, elongated along the axis of the ingot - a longitudinal inhomogeneity. Heterogeneities with scales of ~1μm level out immediately after crystallization [5]. In $A_2^V B_3^{VI}$ crystals, point and line defects are formed, which create additional stresses in them. The homogenization of inhomogeneities such as growth bands occurs much faster after impurity intercalation along the (0001) $A_2^V B_3^{VI}$ plane. This process can be carried out at lower temperatures and at high growth rates.

As characteristics of contacting interlayer nanoobjects and quintets, one can primarily consider their elastic properties. The stresses between the quintets of the $A^V{}_2 B^{VI}{}_3$ crystal lattice also develop during phase transformations, chemical reactions in the interfacial region during crystal growth [6]. The shift of quintets relative to each other occurs easily, as a result of which, under the influence of internal stresses between quintets and nanoobjects weakly coupled to each other, various internal stresses arise.

The plastic deformation of quintets in a layered crystal manifests itself microscopically as a shear without noticeable rotation localized between the telluride planes Te$^{(1)}$-Te$^{(1)}$ $A_2^V B_3^{VI}$ <impurity>. In this case, steps appear on the (0001) surface during the relative slip of the telluride layers, such steps are called "slip lines". In the electron microscopic images, we are considering, we see slip lines with a height that varies from point to point.

The sliding of quintets does not occur simultaneously along the entire sliding plane. This process starts in a limited region of the (0001) plane and propagates through the layers with a finite velocity.

Since we are studying the cleavage planes (simultaneously being the basal planes), it is necessary to take into account the dislocations observed during the growth of crystals of the Bi$_2$Te$_3$(Sb$_2$Te$_3$) type in the analysis. Dislocations in Bi$_2$Te$_3$(Sb$_2$Te$_3$) play a special role in the morphology of their cleavage surface. Ordinary dislocations lead to the formation of steps on the cleavage surface. Splitting, like sliding or twinning, cannot immediately cover a large surface. The cleavage should propagate from one point to another in the form of a crack starting its growth from the initial localized nucleus. The edge of the crack, which bounds the cleavage region, can be represented as a special kind of edge dislocation. Such splitting dislocations "creep" without diffusion in the cleavage plane perpendicular to their Burgers vectors, and a crack opens after the dislocations. Since the crack edges advance gradually, they must be described by a continuous distribution of cleaving dislocations with infinitesimal Burgers vectors. Only the directions of these dislocations and their density have physical meaning. Splitting occurs when a sufficiently large number of lattice dislocations can crawl without diffusion one after another along the same plane. Cleavage dislocations accumulate at the crack tip, just as gliding dislocations accumulate in slip lines.

The cleavage surfaces are not ideally smooth, but usually represent a system of steps almost parallel to the cleavage direction. The steps often converge to form higher steps.

Therefore, for a qualitative explanation of the mechanisms of deformations in $A_2^V B_3^{VI}$ layers, arising under the action of compressive stresses, we took as a basis the provisions set forth in [1, 6–17]. Bi$_2$Te$_3$, with its layered structure, which allows the preparation of very thin plates of uniform thickness by simple successive chipping, was a suitable object of study. For Bi$_2$Te$_3$, the cleavage plane coincides with the basal plane of the crystal and is simultaneously the main slip plane, in which the Burgers vector of dislocations is located. This makes it possible to directly observe the dislocation pattern of this plane in the field of an electron microscope, but so far there are no clear images of such patterns on the (0001) surface of $A_2^V B_3^{VI}$ crystals.

To date, despite the large number of works devoted to the mechanisms of growth and composition of islands, as well as elastic stresses in them, many questions remain open. Great interest in the processes of self-organized growth on the surface in elastically stressed systems is associated with the movement of dislocations and their emergence to the surface and with the possibility of obtaining nanoobjects in interlayers. These features of sliding steps at the micro level must be taken into account.

The interlayer space Te$^{(1)}$-Te$^{(1)}$ $A_2^V B_3^{VI}$ <impurity>, being a dislocation reactor, combines the features inherent in nanoreactors.

The study of deformation and dislocation structures in plastically deformed crystals using electron microscopy methods revealed a close relationship between localization in the form of slip lines and bands [16] and a nonuniform distribution of dislocations in a crystal. Depending on the loading conditions and the structural state of the material, a wide variety of dislocation structures of various spatial scales and morphologies is observed, which indicates the processes of self-organization of dislocations [15–17].

The aim of the work is to reveal the morphological features of the self-organization of nanoobjects associated with their deformation during the growth of layered crystals $A_2^V B_3^{VI}$ <impurity>.

EXPERIMENT AND DISCUSSION

The technique for obtaining samples with nanoobjects between blocks of quintets and studying their morphology using an atomic force microscope (*AFM*) is given in [6].

The production of nanoobjects in the interlayer space is associated with defects, which here are subdivided into structural and impurity ones.

During growth and intercalation, as well as during the self-organization of impurities between layers in layered crystals, stresses can develop due to the difference in the characteristics of nanoobjects and quintets (we mean quintets in the $A_2^V B_3^{VI}$ crystal lattice). Figure 1 shows the crystal structure of Bi_2Te_3, which has a layered structure of the tetradymite type; layers of Bi and Te atoms alternating along the C axis of the rhombohedral lattice are combined into blocks (they are sometimes called sandwiches or quintets) containing five layers each. Inside the block, the atoms are bound by strong covalent interactions, while van der Waals forces act between the quintets, and thus conditions are created for deformation and easy intercalation in the $Te^{(1)}$-$Te^{(1)}$ $A_2^V B_3^{VI}$ interlayers by directed diffusion of impurities of different ionic radii [7]. We have obtained a lot of experimental data confirming this point of view. When the crack tip passes through the subboundary, numerous new steps automatically arise, and their number increases with an increase in the preliminary plastic deformation. Step submicrostructures, visible under a microscope, result from the joining of much smaller elementary steps. At the same time, when steps of the opposite sign meet, they can annihilate.

In most materials, the steps have a curvilinear shape. They run approximately parallel to each other and perpendicular to the successive positions of the crack front. Such a pattern of steps should appear, apparently, with an almost complete isotropy of their surface tension, since the energy of the steps becomes minimal in this case. They rather resemble flat two-dimensional defects, in which the disturbances are large in two directions.

a)   b)
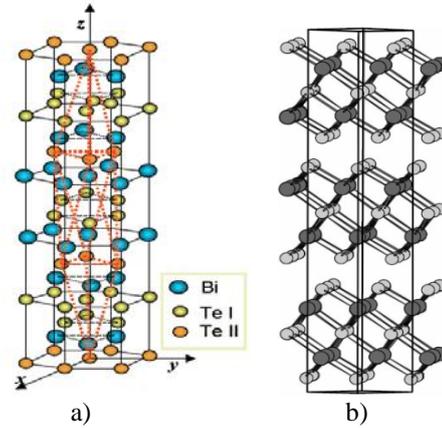
Fig.1. Bi_2Te_3 crystal structure [7]: places $Bi, Te^{(I)}$ and $Te^{(II)}$ are highlighted -a); position of three block quintets -b).
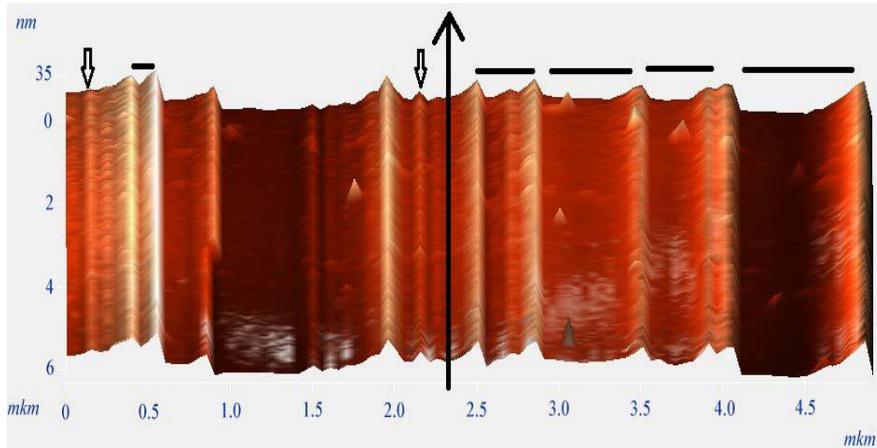
Fig. 2. AFM image of a corrugated structure in the Bi_2Te_3-Cd system: small vertical arrows show small-amplitude corrugations, the black vertical arrow marks the longitudinal direction of the growth of corrugations; horizontal lines on top indicate uneven distances between folds on the surface (0001)

In some materials, steps have a zigzag shape and run along densely packed crystallographic directions [15–16].

Interlayer folds, given in fig. 2-3, can be called corrugated. The mechanism of bending of interlayer nanostructures between blocks can be associated with their elastic stability. In all likelihood, the compressive stress σ exceeds σ_{wx} according to formula (1), the interlayer object bends into folds of a certain size. Forming folds with any wavelength correspond to expression (2).

In the process of formation of nano-objects between telluride quintets in $A_2^V B_3^{VI}$ <impurity> when the equilibrium between them is disturbed, at a certain

critical value of longitudinal compressive forces, small perturbations lead to the formation of dislocations.

Dislocations in layered $A_2^V B_3^{VI}$ crystals can be easily represented by displacing one part of the quintet relative to the other, but not along the entire part of the (0001) plane, but only along its part, as shown in Fig.4. The shear occurs along the helical surface (fig. 4). The value of a single displacement between the $Te^{(1)}$-$Te^{(1)}$ layers is the b-Burgers vector, which reflects both the absolute value of the shear and its direction along the (0001) plane. For layered crystals of the $Sb_2Te_3(Bi_2Te_3)$ type, the vector b lies on the (0001) plane.
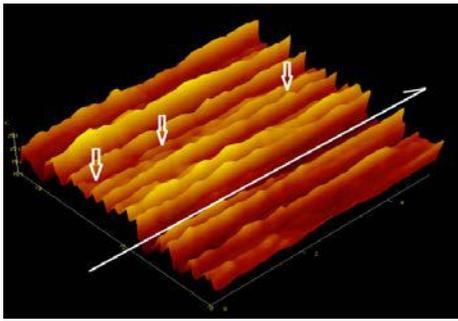
Fig. 3. 3D AFM image of the corrugated Bi_2Te_3-Cu structure: individual corrugations are marked with vertical arrows, the white long arrow shows the direction of crystal growth, which coincides with the longitudinal direction of structure growth. Annealing temperature 700K for 5 hours.

The interlayer space is a region of high dislocation density. Impurity atoms between the $Te^{(1)}$-$Te^{(1)}$ $A_2^V B_3^{VI}$ layers are more inclined to form nanoobjects in defective areas. We consider those dislocations that arise during vertical directional crystallization. In the above diagram (fig. 4) in the studied crystals, internal forces P are indicated, leading to the formation of screw dislocations. These forces are applied to quintets.
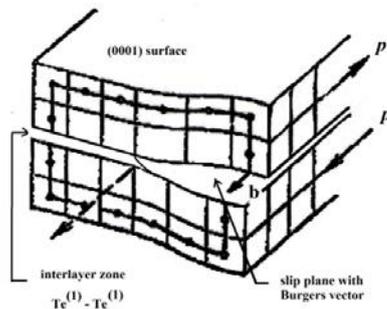
Fig.4. Scheme of a section of a crystal lattice with a screw dislocation in crystals of the Bi_2Te_3 type (b- Burgers vector).

Numerous screw dislocations can emerge on the (0001) surface, which are formed under the influence of internal stresses, for example, during the capture of impurities [17]. Dislocation mounds are formed on the (0001) surface (fig. 5).
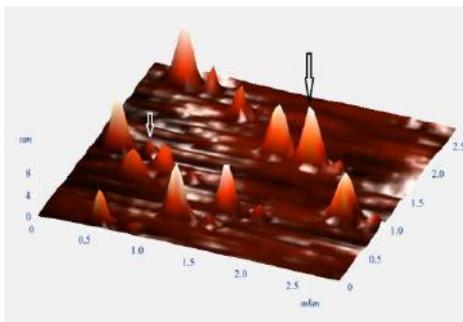
Fig.5. 3D AFM image of locally grown dislocation disordered islands (indicated by arrows) Bi_2Te_3<Zn>.
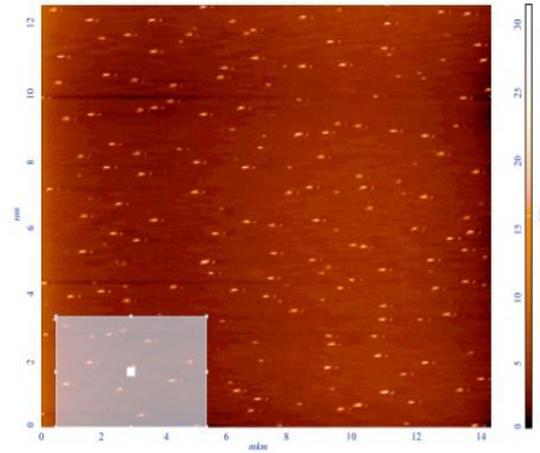
Fig.6. 2D AFM image of ordered Bi_2Te_3<Zn> nanoislands annealed at 500K.
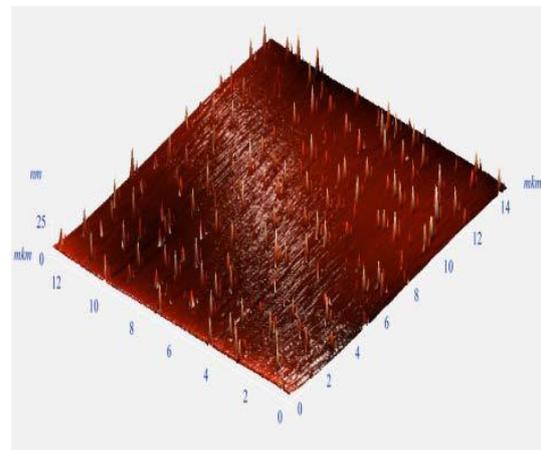
Fig.7. 3D AFM image of ordered nanoislands of (0001) surface in Bi_2Te_3<Zn>

There is competition between dislocation growth mounds, which results in the appearance of a steeper mound. In AFM images, we notice the so-called nanoislands.

Ordered nanoislands were formed on the interlayer surface (0001) by self-organization (see fig. 6). The growth of these nanoobjects can be considered as a manifestation of the mechanism of many dislocation mounds-nanoislands. On the AFM images of the (0001) Bi_2Te_3<Zn> surface in *2D* and *3D* scales (fig. 6), small islands formed by competition near large islands are noticeable. This is the result of the exit of an additional screw dislocation not absorbed by the larger dislocation mound. Such mounds usually have a non-circular shape, they rather resemble elongated ellipses.

The macroscopic bending of the system under consideration leads to an increase in the strain energy of the quintets. Here, stress relaxation mechanisms are possible, leading to the interaction of quintets. These deformations lead to the formation of interlayer folds, steps and mounds with their disintegration into separate nanoislands (fig.5-7).
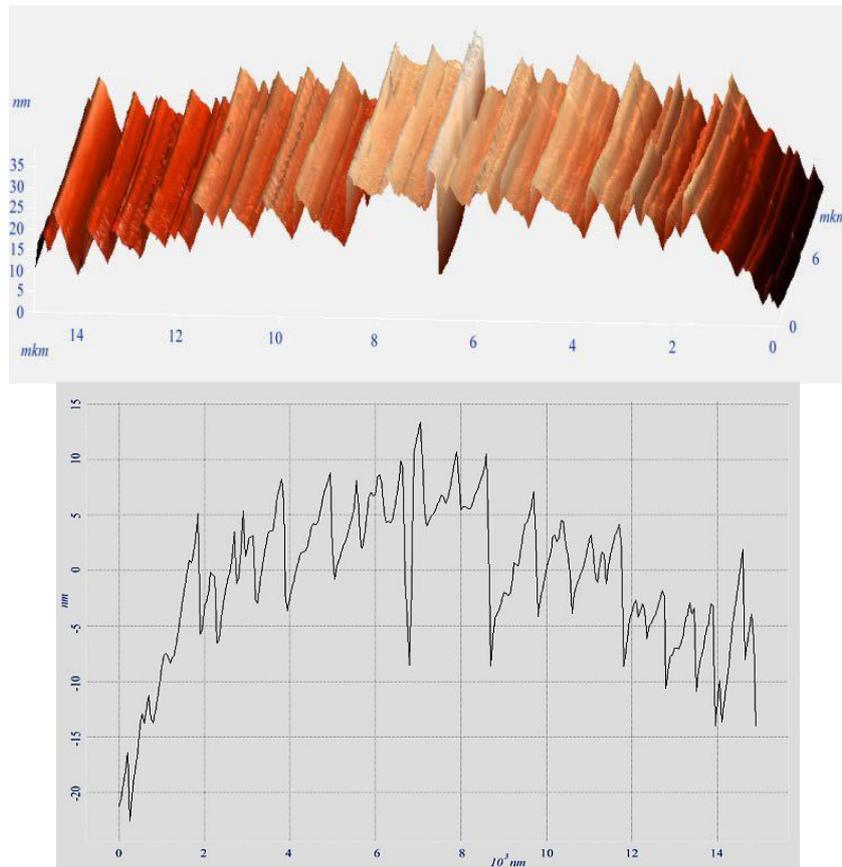
Fig.8. Corrugated structures based on Bi$_2$Te$_3$-Se annealed at 700K.

To compare the corrugated (figs. 2, 3, 8) and stepped structures (fig. 9) obtained by us in $A_2^V B_3^{VI}$ with films [1], various schemes of corrugating films on substrates under the action of stresses are given (see fig. 10). Comparison of the morphology of interlayer nanoformations with the shape of the films from Fig. 10 revealed a certain similarity of corrugations, differing only in wavelength and amplitudes. They arise due to the possible coherent deformation of the structures of nanoobjects and the (0001) $A_2^V B_3^{VI}$<Se, Ni, In> surface. The scheme shown in Fig. 10a from [1] is very close to the real surface morphology (0001) of Bi$_2$Te$_3$<Cu, Cd, Se> and Sb$_2$Te$_3$<In> which are shown in figs. 2, 3 and 12 (a, c, e).

One of the mechanisms for the formation of ordered nanostructures can be faceting, in which a flat crystalline surface is rearranged into a periodic structure of "hills and valleys" to reduce the free energy on the surface. Subsequent heteroepitaxial growth on faceted surfaces under optimized growth conditions leads to the formation of corrugated superlattices [14]. Corrugated structures shown in fig. 2, 3 and 8.

a)   b)   c)   d)
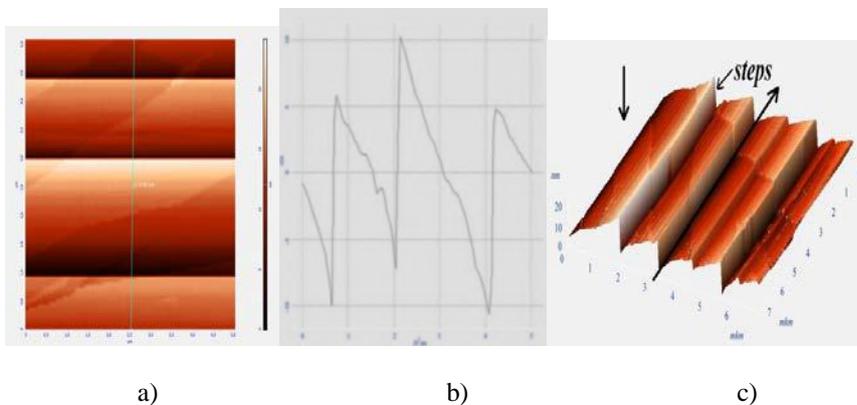
Fig.9. Stepped structures in the Bi$_2$Te$_3$-Ni system: *2D- AFM* scale - a); profilogram along the line shown in fig. a) - b); the direction of crystal growth (large black arrow), the left vertical arrow is the direction of compression of steps - c); a separate fragment of steps without nanoislands (height *h=10nm*) (– d).

17

a)   b)   c)
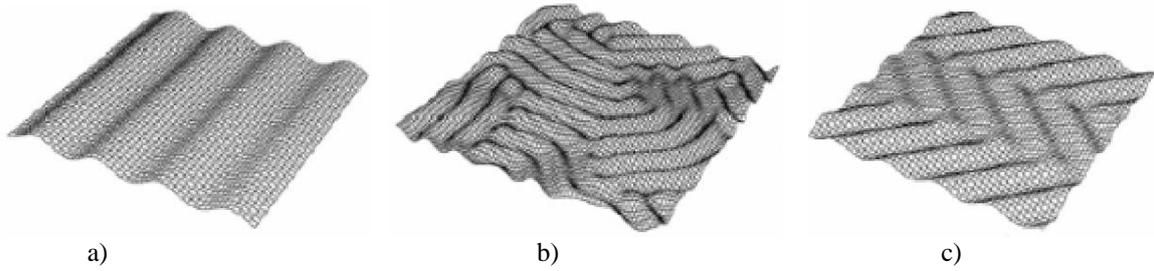
Fig. 10. Various schemes of corrugation of thin films on a substrate under the action of compressive stresses [1]:
a)-stripe structure, b)-labyrinth structures, c)- fir-tree structures.

It is also necessary to take into account the redistribution of mass by plastic shifts in the medium. Areas of increased and reduced mass density (*M*-regions) are formed on inhomogeneities of the distribution function of shear displacements [13]. Displacement inhomogeneities also exist in the Bi_2Te_3 atomic medium, albeit on a much smaller scale. If a significant part of the atoms is involved in the displacements, and these displacements obey certain laws, then we can speak of collective motions. The collective motion of atoms plays a significant role in the plastic deformation of a material. In addition, the collective motion leads to an uneven distribution of atoms in the crystal lattice and is weakened by point and line defects, which are present in abundance in $A_2^V B_3^{VI}$ [5]. Around such defects, it is distorted. In this case, a vacancy can be considered as a compression center, and an interstitial atom as an expansion center in an elastic medium [13]. The wall of vacancies or interstitial atoms will already represent a region of dilatation of the atomic structure. When defects are annihilated, the redistribution of excess and missing mass occurs, and the ideality of the material is restored.

a)   b)   c)
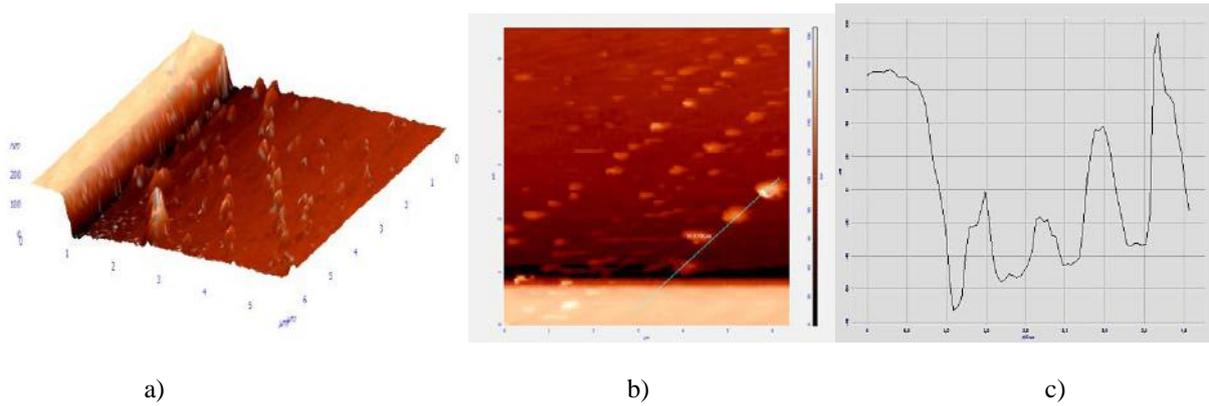
Fig.11. 3D AFM image of stepped structures on the Bi_2Te_3-Cu surface - a), *2D AFM* image of nanoislands on the lower step of the (0001) surface - b), profilogram along the line in fig. b) is shown in fig. - c)

If the substrate cannot accumulate elastic energy, then the nanoobject becomes unstable under any compressive stress, and the wrinkling process is completely determined by kinetics [8–9]. In this case, folds can be formed with any wavelength exceeding a certain critical value [10]:

$$\lambda_c = \pi h \sqrt{-\frac{\overline{E_f}}{3\sigma}} \qquad (4)$$

The thickness (h) of the nanoobjects obtained by us does not exceed several *nm*.

Figures 2, 3, 8 and 12 (a) show the corrugated structures associated with the formed folds. Figure 11 (a, c) shows the wavelengths of folds 20–30 *nm* in size. To compare the folds arising in the substrate-film system [1] with corrugations in the $A_2^V B_3^{VI}$<Se, Ni, Cd, Cu> systems, their figures 2, 3, 8 and 12 are shown. Interlayer steps with nanoislands in the

Bi_2Te_3<Cu > system is shown in fig. 11(a).

It should be noted that the growth of folds with different wavelengths, i.e., an increase in their amplitude, occurs at a crystal growth rate of 1 to 2.5*cm/h*.These changes in amplitudes and wavelengths are reflected in the morphology of the structures shown in fig.12. At the initial stage of deformation, the amplitude growth rate is maximum for folds with a wavelength [11]:

$$\lambda_m = \pi h \sqrt{-\frac{\overline{E_f}}{\sigma}} \qquad (5)$$

Therefore, based on kinetic considerations, at the stage of nucleation on a quintet substrate, rapidly growing folds with a wavelength according to (5) will prevail, which, in contrast to the case of an elastic substrate, is determined only by the characteristics of nanoobjects and the magnitude of compressive stresses.

a)

b)

c)

d)

e)

f)
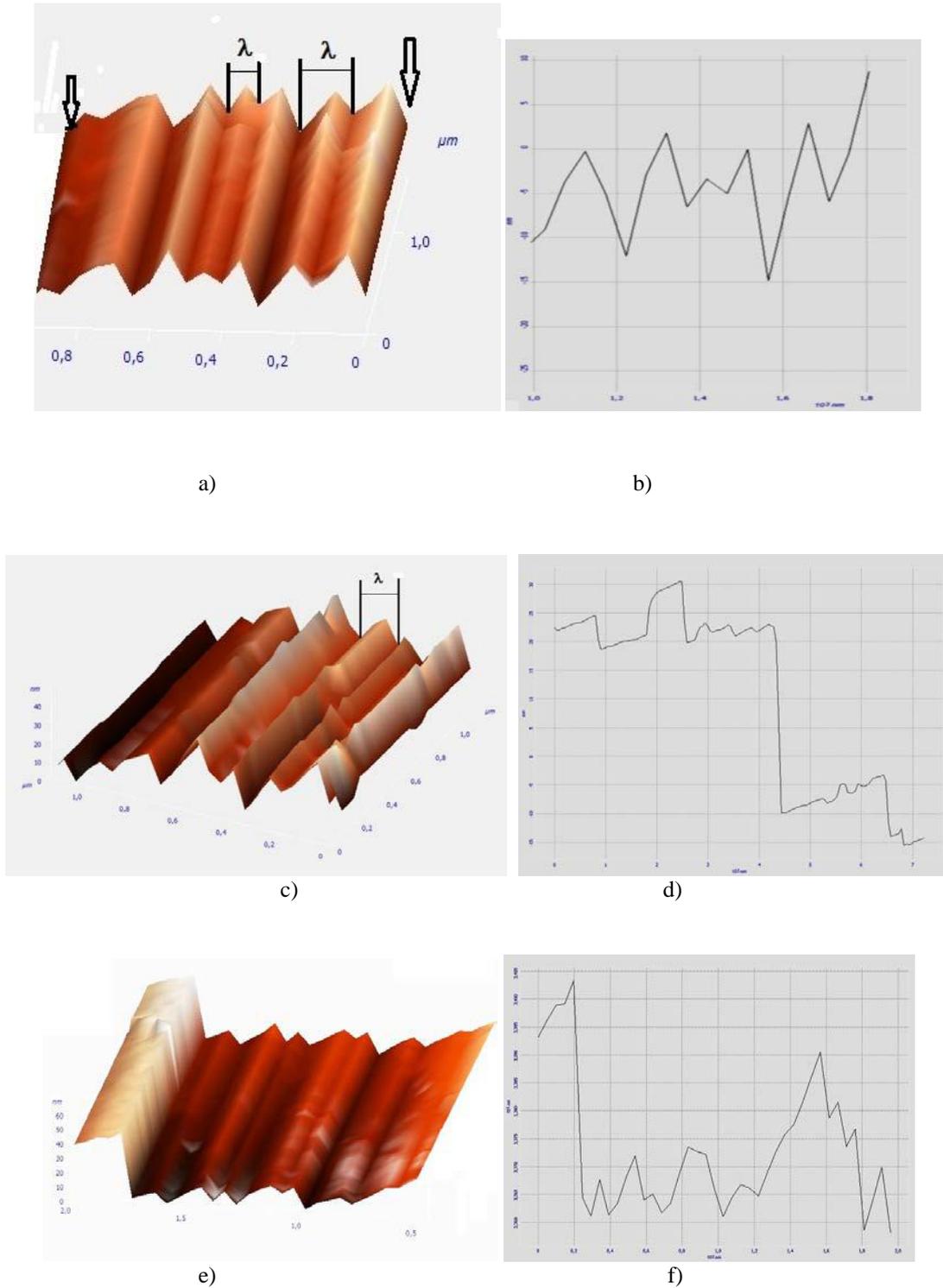
Fig.12. Corrugated structures with nanosteps in the *Sb₂Te₃-In* system:
separately selected lengths of "waves" (λ) of corrugations and directions of their deformations - a);
profilogram-b); corrugation fragment-c); profilogram-d); corrugation with a step on the left - e); profilogram–f.

When the amplitude of the folds with the wavelength λ_m becomes comparable with the film thickness, the process of their growth slows down considerably. The stress value in the film at this stage is determined as [12]:

$$\sigma = -\pi^2 h^2 \qquad (6)$$

i.e. the longer the wavelength of the folds, the stronger the relaxation of compressive stresses. Since the wavelength (see Fig. 12) is large (~20-30) nm, the compressive stresses are high. Therefore, further stress relaxation occurs due to an increase in the wavelength of the folds (coarsening), which is provided by plastic deformation of the quintets. The data from [1, 8, 12 and 15] used to explain the possible deformations in the interlayers made it possible (in figs. 2, 3, 12a) to show the possible directions of deformation during the growth of Sb₂Te₃(Bi₂Te₃)<Cu, Ni, In> crystals.

19

Figures 2 and 3 show the directions of compressive stresses (they are indicated by arrows perpendicular to the direction of the (0001) plane) at the final stage of nanoobject growth during impurity mass transfer in the $Te^{(1)}$-$Te^{(1)}$ $A_2^V B_3^{VI}$ zone. These figures also show the longitudinal directions of growth of corrugated structures.

The coarsening is accompanied by an increase in the amplitude of the folds in accordance with the expression [12]:

$$A = h \sqrt{\frac{1}{3(\frac{\lambda^2}{\lambda_c^2} - 1)}} \qquad (7)$$

From the experimental data, the parameter A was found, which varies within 5 -10 nm depending on the growth rate (1.1 -2.4)cm/h and the crystallization temperature. The parameter A given in [1] differs from the data obtained by us. As shown by our studies, the local places of formation of nanoobjects can be inhomogeneities around screw dislocations and other defect structures such as Te vacancies on the (0001) $A_2^V B_3^{VI}$ surface. Thus, these processes are of a local nature, as evidenced by the formed nanoislands on different parts of the (0001) surface (see figs. 5 and 6). We have developed such technological conditions under which the distribution of internal stresses contributed both to the formation of corrugated structures and nanoislands (for example, figs. 5 and 6).

When discussing the results obtained, the process of plastic deformation of the (0001) surface of quintets should not be left aside. It is necessary to take into account the factor that plastic deformation in general is a process of local mass displacement. For any type of defect, plastic shear is a section of the shear plane, in which shear displacements are greater than in neighboring sections of the shear plane, where the deformation is considered elastic. The mass displaced by plastic shears is commensurate with the extraplane mass, and for a completed shear it is equal to it. The displaced mass is 3–4 orders of magnitude higher than that given by the calculation based on the elastic energy of dislocations [13]. Such a plastic shear occurs between $Te^{(1)}$-$Te^{(1)}$ $A_2^V B_3^{VI}$ and creates additional (0001) planes of sheared steps, similar to the surfaces shown in Figs. 2 and 9. With shifts occurring only along one slip plane of a bismuth telluride crystal, as described in [5], the dislocations are arranged in the form of parallel lines. They are also responsible for the stresses created across the layers and causing folds (corrugations). The formation of corrugations and their movement are analogous to the movement of dislocations.

The intensity of mass transfer, which leads to the formation of folded structures and three-dimensional nanoislands, increases with an increase in the growth rate during diffusion intercalation. In this case, the intercalated atoms can be fixed at the exit points of screw dislocations, forming nanoislands (these sliding points are marked in fig. 4).

It is believed that the key factor in the transition to the three-dimensional island growth of nanoobjects is the energy gain due to the reduction of stresses in 3D islands through their elastic relaxation. On a sufficiently clean surface, interlayer volumetric islands are not formed, and the growth of nanoobjects occurs due to the movement of steps (step-layer growth) (see fig. 9 c, d). The steps shown in Fig. 9(c, d) can arise both during the formation of two-dimensional nuclei and when a screw dislocation in Bi_2Te_3 reaches the surface with accumulation of easily diffusible impurities (Cu, Ni, Zn, Se). It is possible that the structure of the stepped surface is related to the layer-by-layer mechanism of growth. Moreover, the steps are quite large: ~10nm, formed as a result of the merging of small steps.

The morphology of nanoobjects intercalated at temperatures (600 and 700K) and grown at growth rates (1.1 and 2.4cm/h) made it possible to draw the appropriate conclusions. Depending on the growth rate, interlayer folded-corrugated structures and ordered nanoislands were grown. The formation of interlayer microstructures is influenced by internal interlayer stresses, which lead to elastic interaction with the formation of various types of nanoobjects. AFM images in 2D and 3D scales indicate the formation of stable steps, folds (corrugated structures with a wavelength of 20-30nm) and three-dimensional ordered nanoislands ~ 5-8nm high. Internal stresses play a significant role in the development of 3D islands and their size distribution (see fig. 5-7). Stresses and mass transfer lead to a non-periodic distribution of corrugations on the surface (0001) $A_2^V B_3^{VI}$ <impurity>. To control the periodicity of the formation of nano-objects, nanoislands, their adhesion with subsequent corrugation, it is necessary to carry out annealing.

CONCLUSIONS

The surface morphology of interlayer corrugated structures in $A^V_2 B^{VI}_3$ <impurity> type crystals and corrugated thin films on substrates under compressive stresses is identical. Comparison of the calculated parameters of the wavelength and amplitude of the corrugations in this case was of a qualitative nature. Flaking due to elastic deformation in the interlayer space $Te^{(1)}$-$Te^{(1)}$ $A_2^V B_3^{VI}$ should not be observed due to the closed space in which nanoobjects are located. *AFM* images of nanoformations of various shapes indicate the processes of compression and tension between quintets in layered structures. In all likelihood, helical dislocation mounds play a special role in the mechanism of self-organization of interlayer nanoobjects.

The formed interlayer structures in $A^V_2 B^{VI}_3$ <impurity> have important technical applications in thermoelectricity.

[1] *A.R. Shugurov, A.V. Panin.* Mechanisms of periodic deformation of the "film-substrate" system under the action of compressive stresses. Physical mesomechanics, Russia, 2009, 12, 3, pp.23-32.

[2] *G.C.A.M. Janssen, A.J. Dammers, V.G.M. Sivel, W.R. Wang.* Tensile stress in hard metal films. Appl. Phys. Lett. 2003,v.83, №16, pp.3287-3289.
doi. org/10.1063/1.1619561.

[3] *H.G. Allen, B.G. Neal.* Analysis and design of structural sandwich panels. Oxford-NY:Pergamon Press, 1969, pp. 292.

[4] *J. Groenewold.* Wrinkling of plates coupled with soft elastic media. Physica A: Statistical Mechanics and its Applications. Elsevier, 2001,vol. 298(1), pp.32-45.
DOI: 10.1016/S0378-4371(01)00209-6.

[5] *B.M. Goltsman, V.A. Kudinov, I.A. Smirnov.* Semiconductor thermoelectric materials based on Bi_2Te_3. Ed. Nauka, Moscow, 1972, pp.320.

[6] *F.K. Aleskerov, K.Sh. Kahramanov, S.Sh. Kahramanov.* Percolation Effect in Copper and Nickel_Doped Bi_2Te_3 Crystals. Inorganic Materials, 2012, v.48, №5, pp. 456–461.

[7] *A.V. Shevelkov.* Chemical aspects of creation of thermoelectric materials. Advances in Chemistry (Russia), 2008, 77 (1), pp. 3-21.

[8] *R. Huang, Z. Suo.* Instability of a compressed elastic film on a viscous layer. International Journal of Solids and Structures, 2002, v.39. №7, pp.1791-1802.

[9] *N. Sridhar, D.J. Srolovitz, B.N. Cox.* Buckling and post-buckling kinetics of compressed thin films on viscous substrates. Acta Materialia. 2002, v.50, №10, pp.2547-2557. DOI: 10.1016/S1359-6454(01)00446-3

[10] *R. Huang, S.H. Im.* Evolution of wrinkles in elastic-viscoelastic bilayer thin films. J. Appl. Mech. 2005,v.72, №6. pp.955-961. doi.org/10.1115/1.2043191.

[11] *R. Huang.* Kinetic wrinkling of an elastic film on a viscoelastic substrate. Journal of Mechanics and Physics of solids. 2005,v.53, №1, pp. 63-89.
doi:10.1016/j.jmps.2004.06.007.

[12] *R. Huang, S.H. Im.* Dynamics of wrinkle growth and coarsening in stressed thin films. Phys. Rev. E. 2006, v.74, №2. pp.026214-12. doi.org/10.1103/PhysRevE. 74.026214.

[13] *A.V. Markidonov, T.A.Tikhonov, V.V. Neverov.* Mass displacement by plastic shifts. Fundamental problems of modern materials science, Russia, 2007, vol. 4, №.2, pp.41-46.

[14] *Zh.I. Alferov.* The history and future of semiconductor heterostructures. Semiconductors. 1998, v.32, pp.1-14. doi.org/10.1134/1.1187350.

[15] *G.A. Malygin.* Dislocation Self-Organization and Slip Localization in Crystals Undergoing Plastic Deformation. Physics of the Solid State, 1995, v.37, №1, pp.1-19.

[16] *J. Friedel.* Dislocations. Pergamon, Oxford, 1964.

[17] *L.N. Rashkovich.* How crystals grow in solution. Soros Educational Journal, Physics (Russia), 1996, №3, pp. 95-103.